

Supporting Information

Zinc-Nickel-Cobalt Ternary Hydroxide Nanoarrays for High- Performance Supercapacitors

Zi-Hang Huang,¹ Fang-Fang Sun,¹ Munkhbayar Batmunkh,² Wen-Han Li,¹ Hui Li,¹ Ying Sun,¹ Qin
Zhao,¹ Xue Liu,¹ Tian-Yi Ma^{3,*}

¹Institute of Clean Energy Chemistry, Key Laboratory for Green Synthesis and Preparative
Chemistry of Advanced Materials, College of Chemistry, Liaoning University, Shenyang 110036,
China

²Australian Institute for Bioengineering and Nanotechnology, University of Queensland, St. Lucia,
QLD, 4072 Australia

³Discipline of Chemistry, University of Newcastle, Callaghan, NSW 2308, Australia

* Corresponding authors: Tian-Yi Ma, Tianyi.Ma@newcastle.edu.au

1. Calculations

1.1 Capacitances of single electrode

The areal and gravimetric capacitance of a single electrode can be calculated based on galvanostatic charge-discharge experiments according to Equation S1 and S2:

$$C_s = \frac{I \times t}{\Delta U \times S} \quad (\text{Equation S1})$$

$$C_m = \frac{I \times t}{\Delta U \times m} \quad (\text{Equation S2})$$

where C_s and C_m (mF cm⁻² or F g⁻¹) are the areal and gravimetric capacitance, I is the discharge current (mA), t is the time (s), ΔU is the potential window (V), S is the working area of electrode (cm²), m is the mass of active material.

1.2 Capacitances of ASC Devices

The volumetric capacitance (C_V , unit in F cm⁻³) of the Zn-Ni-Co TOH-130//FEG device can be calculated based on galvanostatic charge-discharge experiments according to Equation S3:

$$C_V = \frac{I \times t}{U \times V} \quad (\text{Equation S3})$$

where I is the charge-discharge current (A), t is the discharge time (s), U is the operating voltage and V is the total volume (cm³) of the whole device stack including two electrodes, electrolyte-soaked separator, as well as the package.

The gravimetric capacitance of ASC device can be calculated based on galvanostatic charge-discharge experiments according to Equation S4:

$$C_M = \frac{I \times t}{U \times m} \quad (\text{Equation S4})$$

where C_M (F g⁻¹) is the gravimetric capacitance of the ASC, I is the discharge current (mA), t is the time (s), U is the operating voltage of the ASC (V), m is the mass of the total mass of active material.

1.3 Volumetric energy density and power density of Zn-Ni-Co TOH-130//FEG Devices

Volumetric energy density (E , Wh cm⁻³) and power density (P , W cm⁻³) of the devices are calculated using the following equations:

$$E_V = \frac{C_V \times U^2}{2 \times 3600} \quad (\text{Equation S5})$$

$$P_V = \frac{3600 \times E_V}{t} \quad (\text{Equation S6})$$

Where C_V (F cm⁻³) is the specific capacitance, U is the operating voltage (V) and t is the discharge time (s).

Gravimetric energy density (E , Wh/kg) and power density (P , W/kg) are calculated using the following two equations:

$$E_M = \frac{1000 \times C_M \times U^2}{2 \times 3600} \quad (\text{Equation S7})$$

$$P_M = \frac{3600 \times E_M}{t} \quad (\text{Equation S8})$$

where C_M (F/g) is the gravimetric capacitance of SSC device, U is the operating voltage (V) and t is the discharge time (s).

1.4 Charge balance for Zn-Ni-Co TOH-130//FEG Devices

To achieve the maximum and stable performance of the ASC device, the capacity (Q) of negative and positive electrode should be balanced, *i.e.*,

$$Q_- = Q_+ \quad (\text{Equation S9})$$

The capacity is associated with areal capacitance (C_s), potential window (ΔU) and working area of electrode (S), as shown in Equation S8:

$$Q = C_s \times \Delta U \times S \text{ (Equation S10)}$$

Combining Equation S9 and S10, the areal capacitance of negative electrode to positive electrode should satisfy Equation S11:

$$\frac{C_{s,-}}{C_{s,+}} = \frac{(S_+) \times (\Delta U_+)}{(S_-) \times (\Delta U_-)} \text{ (Equation S11)}$$

In our work, we fixed the working area of both electrodes at 1.0 cm². Substitute $\Delta U_- = 1.2$ V and $\Delta U_+ = 0.6$ V. According to Equation S11, the ratio of areal capacitance of FEG to Zn-Ni-Co TOH-130 electrode is ~0.5, which is close to the areal capacitance of FEG (1.07 F cm⁻²) to Zn-Ni-Co TOH-130 (2.14 F cm⁻²) used in our work.

2. Supplementary Figures and Tables

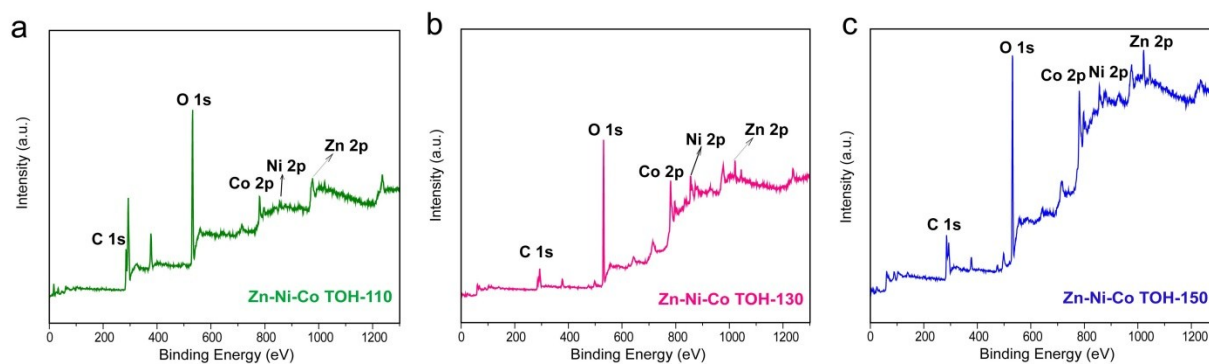


Fig. S1 XPS survey spectrum of (a) Zn-Ni-Co TOH-110, (b) Zn-Ni-Co TOH-130, and (c) Zn-Ni-Co TOH-150 electrodes.

Table S1 Atomic percentage (%) of zinc, nickel, and cobalt in Zn-Ni-Co TOH

Sample Name	Zn (%)	Ni (%)	Co (%)
Zn-Ni-Co TOH-110	1.08	1.91	3.72
Zn-Ni-Co TOH-130	2.32	6.26	12.09
Zn-Ni-Co TOH-150	2.40	1.90	4.02

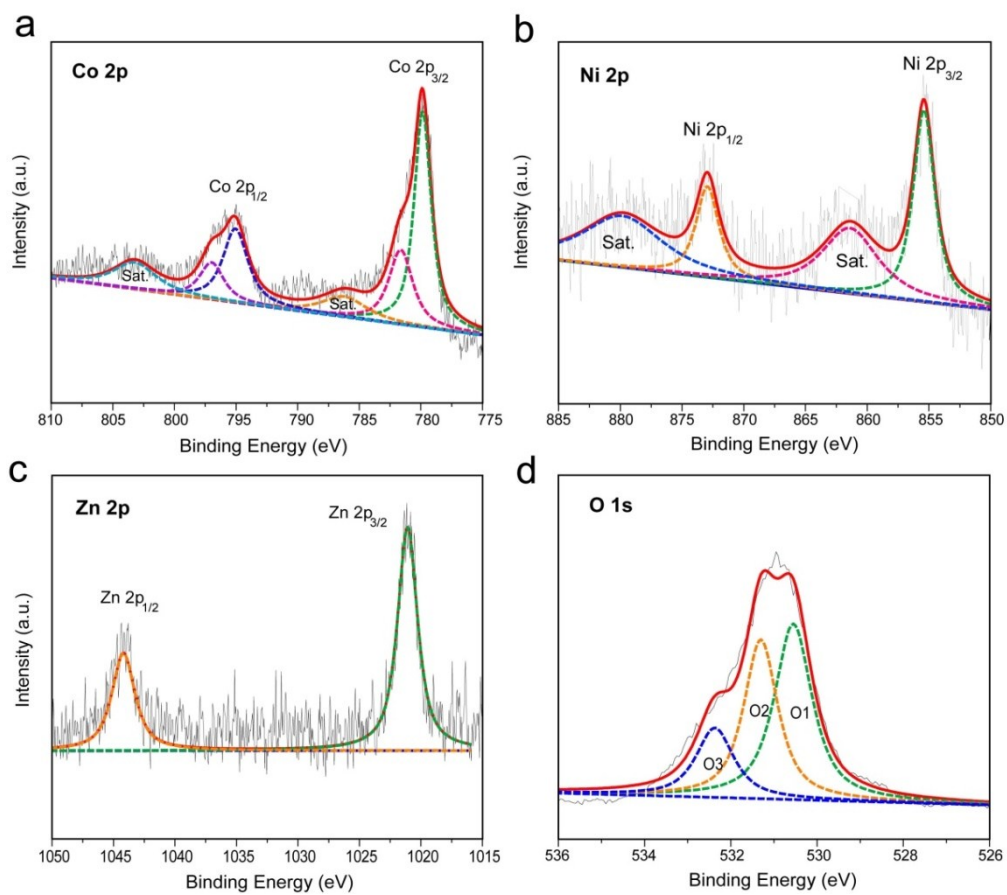


Fig. S2 XPS analysis of Zn-Ni-Co TOH-110 sample: high resolution (a) Co 2p XPS peak, (b) Ni 2p XPS peak, (c) Zn 2p XPS peak and (d) O 1s XPS peak. Peak separations are highlighted and labelled.

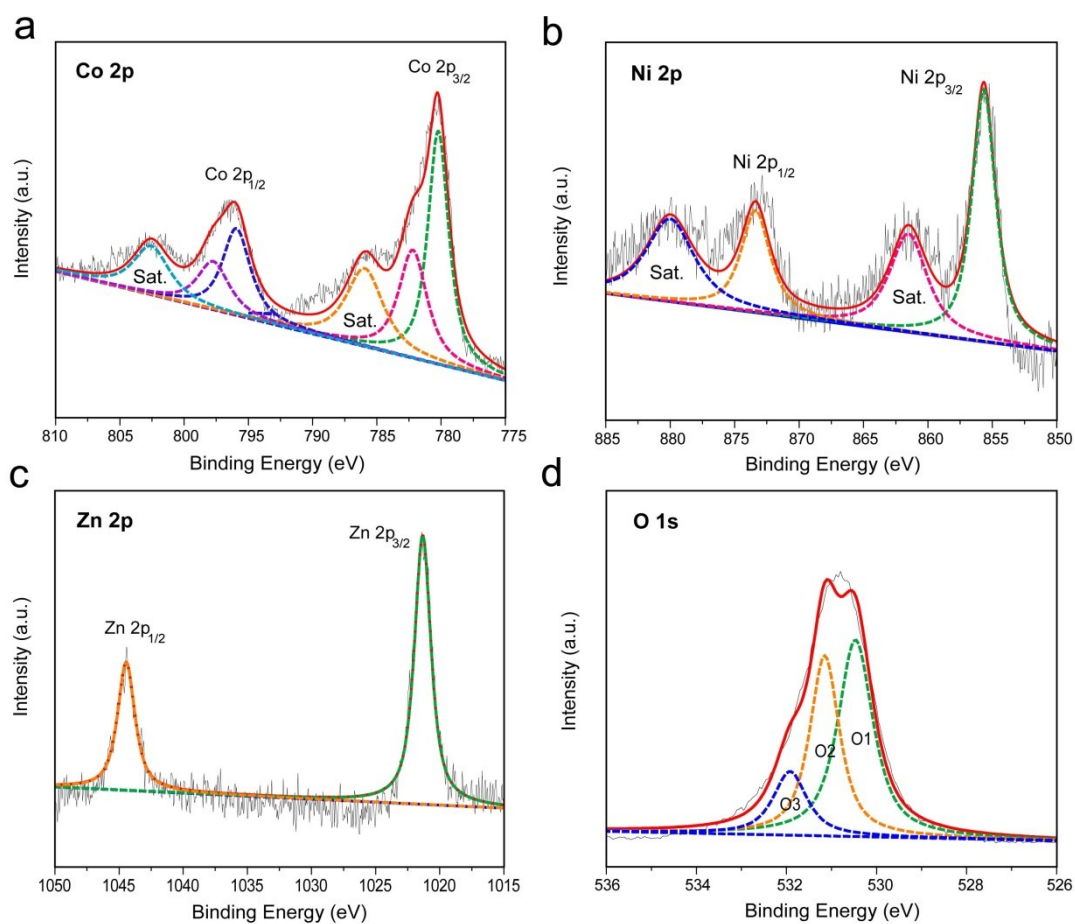


Fig. S3 XPS analysis of Zn-Ni-Co TOH-150 sample: high resolution (a) Co 2p XPS peak, (b) Ni 2p XPS peak, (c) Zn 2p XPS peak and (d) O 1s XPS peak. Peak separations are highlighted and labelled.

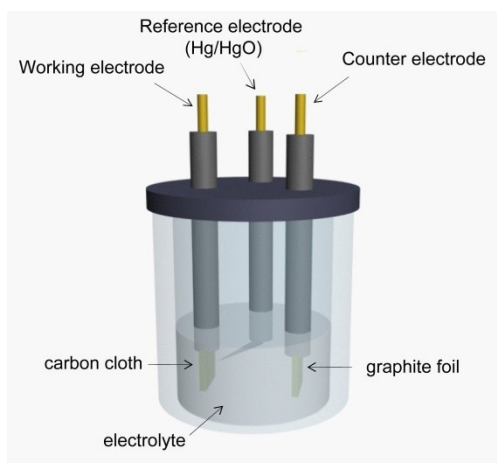


Fig. S4 Schematic illustration of the three-electrode cell used in this work for the electrochemical measurements.

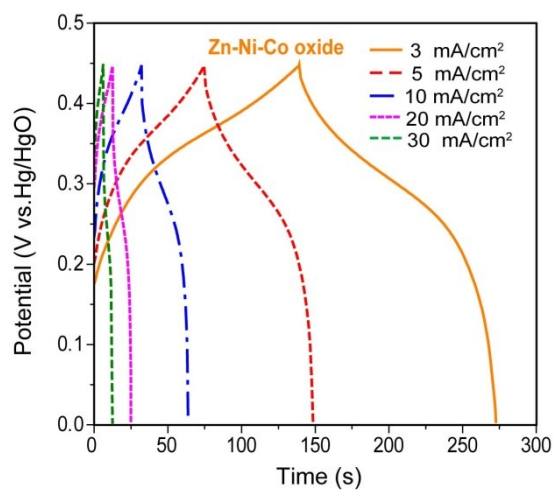


Fig. S5 Galvanostatic charge-discharge (GCD) profiles of Zn-Ni-Co oxide electrode collected at various current densities.

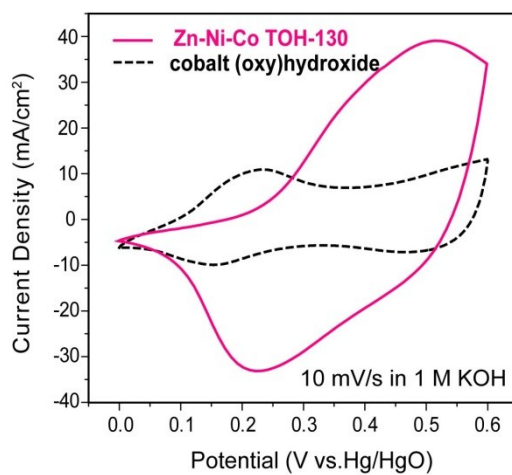


Fig. S6 Cyclic voltammogram (CV) curves of Zn-Ni-Co TOH-130 and cobalt (oxy)hydroxide electrodes measured at a scan rate of 10 mV s⁻¹.

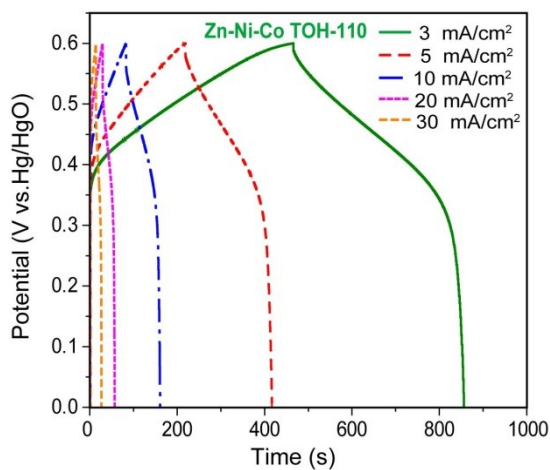


Fig. S7 GCD profiles of Zn-Ni-Co TOH-110 electrode collected at various current densities.

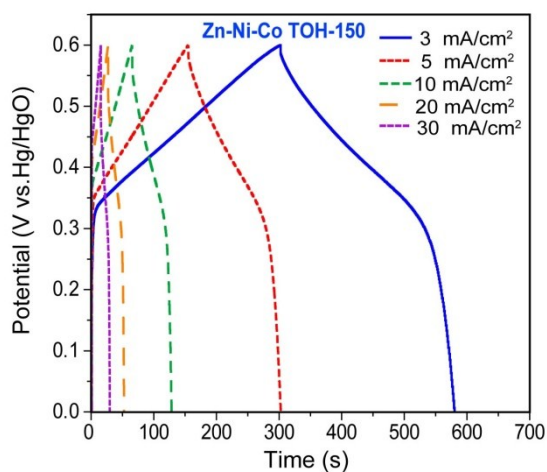


Fig. S8 GCD profiles of Zn-Ni-Co TOH-150 electrode collected at various current densities.

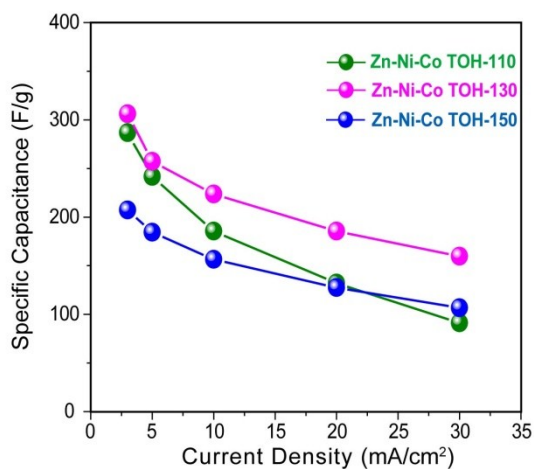


Fig. S9 Gravimetric capacitance of the three Zn-Ni-Co TOH-based electrodes measured at different current densities in the potential range of 0~0.6 V vs. Hg/HgO.

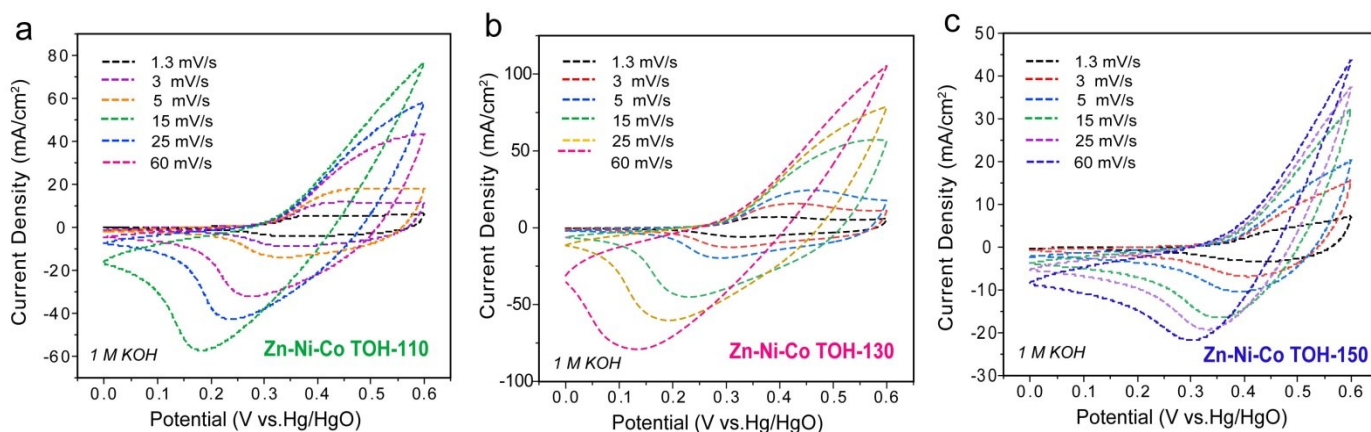


Fig. S10 CV curves of the Zn-Ni-Co TOH-110 (a), Zn-Ni-Co TOH-130 (b), and Zn-Ni-Co TOH-150 (c) electrodes measured at different scan rates.

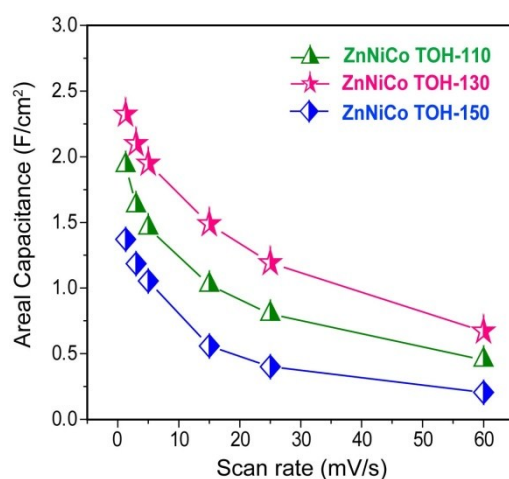


Fig. S11 Areal capacitance of the three Zn-Ni-Co TOH-based electrodes measured by CV at different scan rates (1.3 mV s^{-1} to 60 mV s^{-1}) in the potential window of 0~0.6 V.

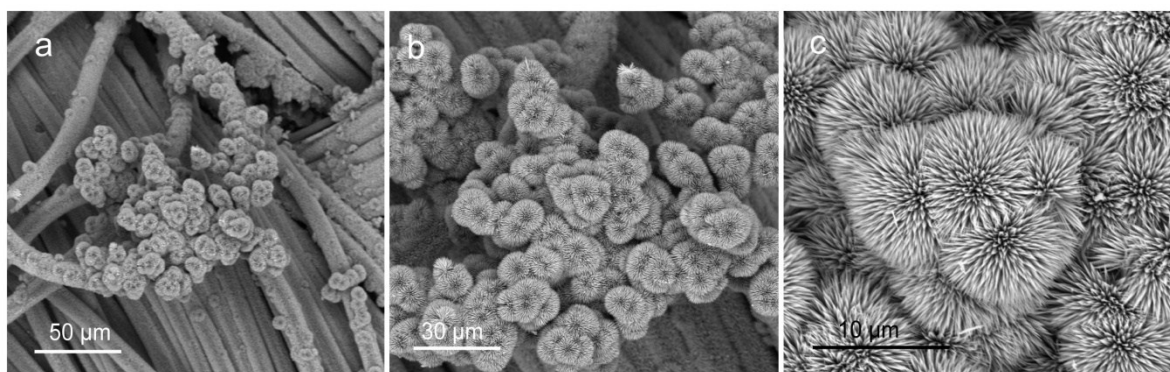


Fig. S12 SEM images of Zn-Ni-Co TOH obtained at $130 \text{ }^\circ\text{C}$ for 12 h.

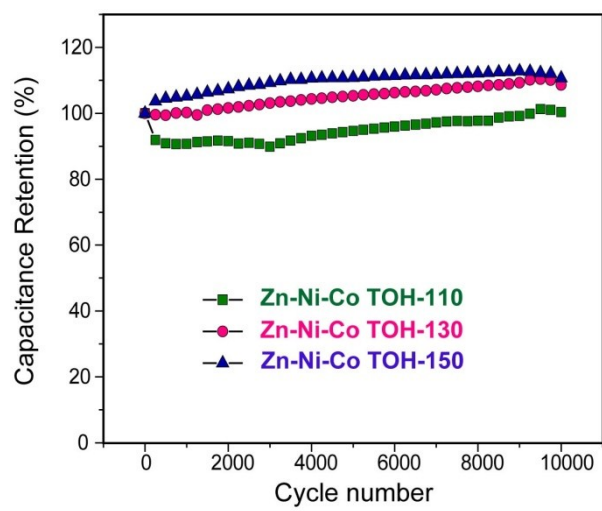


Fig. S13 Cyclic stability of the Zn-Ni-Co TOH-based electrodes tested at a scan rate of 100 mV s⁻¹

3. Electrochemical performance of functionalized partial-exfoliated graphite (FEG)

The electrochemical performances of the FEG electrode was conducted in a three electrode cell containing 1 M KOH electrolyte with Hg/HgO electrode as the reference electrode and graphite foil as the counter electrode. Fig. S14a shows the CV curves for the FEG collected at different scan rates. As can be seen, no significant distortion was observed from the CV curves with the increase of scan rate, suggesting a good rate capability. Fig. S14b provides the galvanostatic charge-discharge curves recorded at various current densities of 3-30 mA cm⁻². Based on the galvanostatic charge-discharge curves collected at 3 mA cm⁻², the areal capacitance of FEG was determined to be 1.07 F cm⁻². Importantly, the electrode retained 80% of its areal capacitance when the current density increases 10 times (Fig. S15). The high capacitance and good rate capability of FEG anode, as well as those of the Zn-Ni-Co TOH-130 cathode, ensure the excellent overall electrochemical performance of the Zn-Ni-Co TOH-130//FEG ASC.

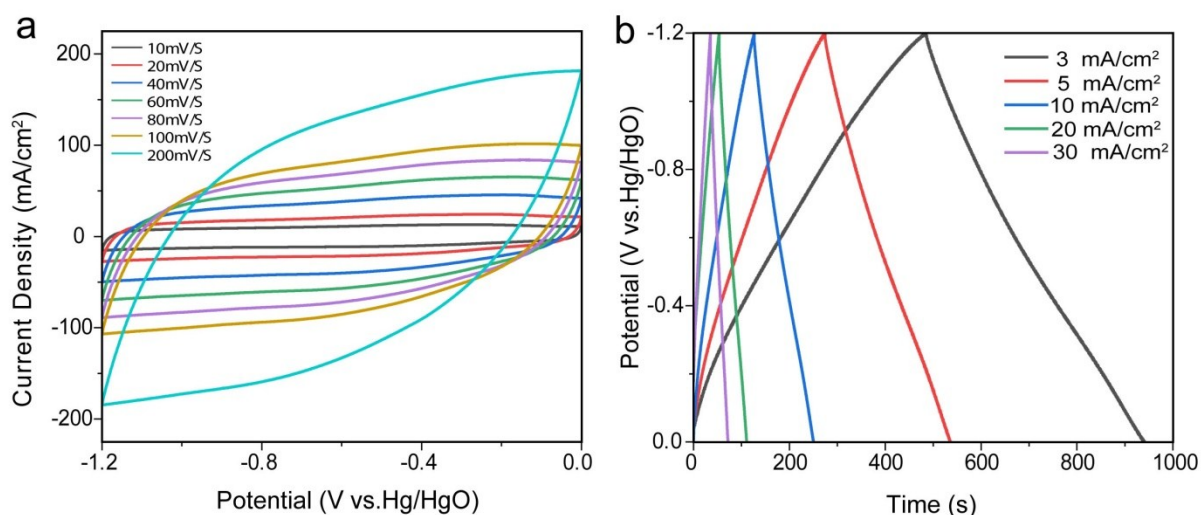


Fig. S14 (a) CV curves of the FEG electrode measured at different scan rates. (b) GCD profiles of FEG collected at various current densities.

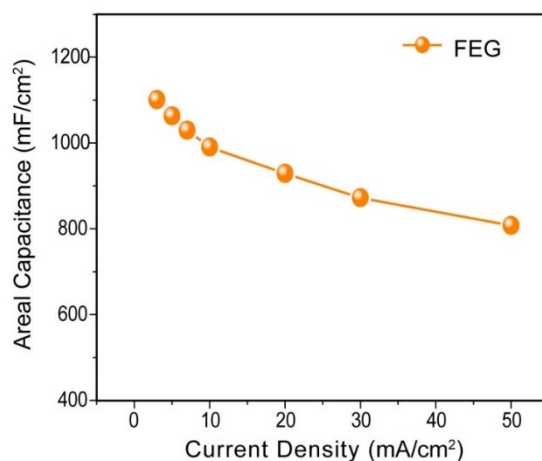


Fig. S15 Areal capacitance of FEG measured at different current densities.

Table S2 Energy storage behaviors of Zn-Ni-Co TOH-130//FEG and recently reported SSC and ASC devices

<i>Device^{a)}</i>	<i>Energy density^{b)}</i>	<i>Cycling Stability</i>	<i>References</i>
V ₂ O ₅ /CNTs//V ₂ O ₅ /CNTs	1.47 mWh cm ⁻³ at 0.005 W cm ⁻³	91.2% (5 000 cycles)	1
MnO ₂ //Fe ₂ O ₃	0.4 mWh cm ⁻³ at 0.055 W cm ⁻³	81.6% (5 000 cycles)	2
V ₃ O ₇ NWs//V ₃ O ₇ NWs	-	85% (5 000 cycles)	3
3D graphene/PPy and graphene/MnO ₂	1.23 mWh cm ⁻³ at 0.0045 W cm ⁻³	90.2% (10 000 cycles)	4
V ₂ O ₅ /H-WO ₃ //V ₂ O ₅ /H-WO ₃	0.09 mWh cm ⁻³ at 0.0003 W cm ⁻³	100% (7 000 cycles)	5
VO _x ·yH ₂ O//VO _x ·yH ₂ O	-	100% (1 000 cycles)	6
Ni(OH) ₂ /NGP//Mn ₃ O ₄ /NGP	0.35 mWh cm ⁻³ at 0.006 W cm ⁻³	83% (12 000 cycles)	7
MnO ₂ /graphene//GH/CW	0.9 mWh cm ⁻³ at 0.0081 W cm ⁻³	90% (10 000 cycles)	8
MnO ₂ NW//Fe ₂ O ₃ NT	0.55 mWh cm ⁻³ at 0.02 W cm ⁻³	84% (5 000 cycles)	9
MnO ₂ @graphene//V ₆ O _{13-x} nanowires	0.87 mWh cm ⁻³ at 0.009 W cm ⁻³	91% (5 000 cycles)	10
MnO ₂ /CC//PPy/FCC	0.8 mWh cm ⁻³ at 0.01285 W cm ⁻³	86% (5 000 cycles)	11
CNT/MnO ₂ //CNT/PPy	0.31 mWh cm ⁻³ at 0.004 W cm ⁻³	85% (5 000 cycles)	12
Zn-Ni-Co TOH-130//FEG	2.43 mWh cm⁻³ at 0.006 W cm⁻³ 1.29 mWh cm⁻³ at 0.18 W cm⁻³	153% (10 000 cycles)	This work

Note: ^{a)} CNTs: carbon nanotubes; MWCNTs: Multi-walled carbon nanotubes; H-WO₃: hydrogenated-WO₃; GH/CW: graphene hydrogel wrapped copper wire; NGP: Ni/graphite/paper; CC: carbon cloth; FCC: functionalized carbon cloth; ^{b)} “-” means not reported.

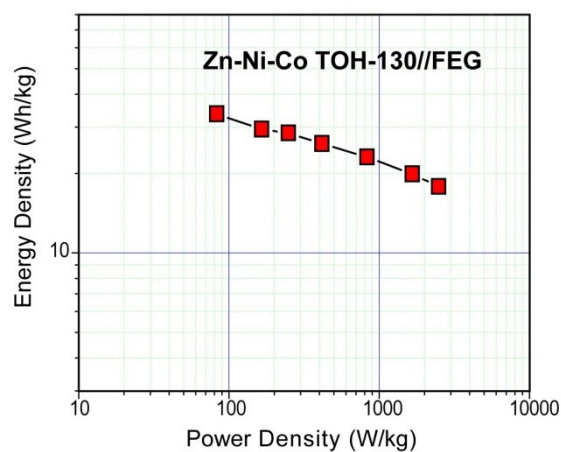


Fig. S16 The gravimetric energy density and power density of the ASC device.

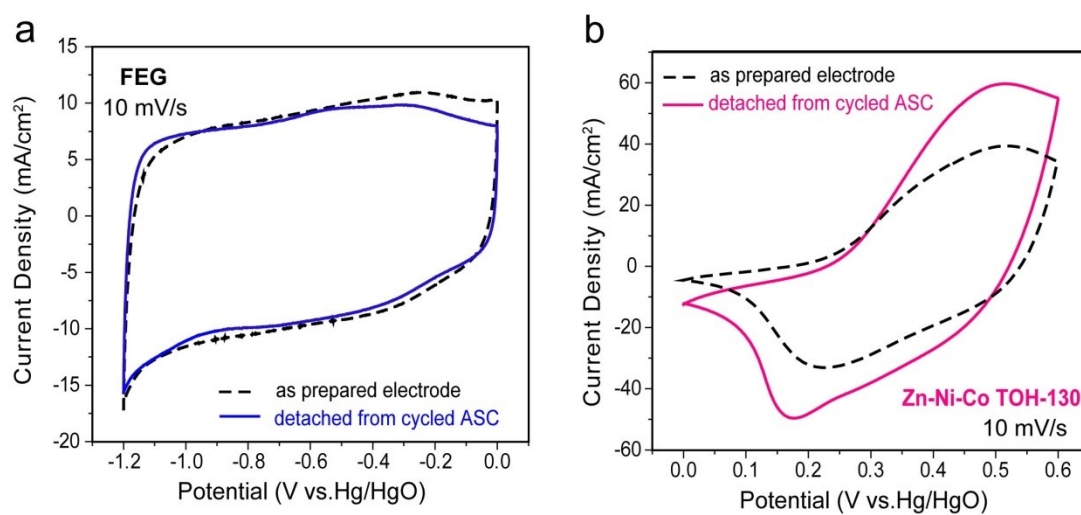


Fig. S17 CV curves of FEG (a) and Zn-Ni-Co TOH-130 (b) for the as prepared electrodes and those detached from cycled Zn-Ni-Co TOH-130//FEG.

References

- 1 G. Yilmaz, C. X. Guo, X. M. Lu, *ChemElectroChem* 2016, **3**, 158-164.
- 2 X. H. Lu, Y. X. Zeng, M. H. Yu, T. Zhai, C. L. Liang, S. L. Xie, M. Balogun, Y. X. Tong, *Adv. Mater.* 2014, **26**, 3148-3155.
- 3 G. M. Wang, X. H. Lu, Y. C. Ling, T. Zhai, H. Y. Wang, Y. X. Tong, Y. Li, *ACS Nano* 2012, **6**, 10296-10302.
- 4 Z. Zhang, K. Chi, F. Xiao, S. Wang, *J. Mater. Chem. A* 2015, **3**, 12828-12835.
- 5 F. M. Wang, Y. C. Li, Z. Z. Cheng, K. Xu, X. Y. Zhan, Z. X. Wang, J. He, *Phys. Chem. Chem. Phys.* 2014, **16**, 12214-12220.
- 6 C. J. Cheng, S. J. Bao, C. M. Li, *Mater. Lett.* 2014, **120**, 283-286.
- 7 J. X. Feng, S. H. Ye, X. F. Lu, Y. X. Tong, G. R. Li, *ACS Appl. Mater. Interfaces* 2015, **7**, 11444-11451.
- 8 Z. Zhang, F. Xiao, S. Wang, *J. Mater. Chem. A* 2015, **3**, 11215-11223.
- 9 P. H. Yang, Y. Ding, Z. Y. Lin, Z. W. Chen, Y. Z. Li, P. F. Qiang, M. Ebrahimi, W. J. Mai, C. P. Wong, Z. L. Wang, *Nano Lett.* 2014, **14**, 731-736.
- 10 T. Zhai, X. H. Lu, Y. C. Ling, M. H. Yu, G. M. Wang, T. Y. Liu, C. L. Liang, Y. X. Tong Y. Li, *Adv. Mater.* 2014, **26**, 5869-5875.
- 11 D. Y. Feng, Y. Song, Z. H. Huang, X. X. Xu, X. X. Liu, *J. Power Sources* 2016, **324**, 788-797.
- 12 Q. Q. Tang, M. M. Chen, C. Y. Yang, W. Q. Wang, H. Bao, G. C. Wang, *ACS Appl. Mater. Interfaces* 2015, **7**, 15303-15313.